Semnan University

Progress in Engineering Thermodynamics and Kinetics Journal

Journal homepage: https://jpetk.semnan.ac.ir/

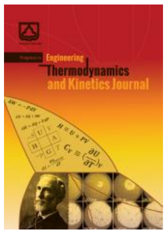

Research Article

Roles of Acidic Deep Eutectic Solvents in Synthesis of Silica Nanoparticle

Maryam Daraee*[a], Mohammad Daraee[b], Ata Feyzizadeh[c]

[a]*Nano Compound Seman Dara Company, Mahdishahr, Semnan, Iran*

[b]*School of Material Engineering and Metallurgy, Semnan University, Semnan, Iran*

[c]*School of Advanced Technologies, Iran University of Science & Technology, Tehran, Iran.*

ARTICLE INFO

Article history:

Received: 202*-**-**

Revised: 202*-**-**

Accepted: 202*-**-**

Keywords:

Acidic Deep Eutectic Solvents

Nano-silica

ChCl

Nanostructure.

ABSTRACT

This article examined the preparation and production of silica nanoparticles using the sol-gel method with two types of deep eutectic solvents (DESs). The DESs were synthesized from choline chloride, urea, and citric acid. To determine the physicochemical properties of the nano-silica, X-ray diffraction, Fourier transform infrared spectroscopy, scanning electron microscopy, energy-dispersive X-ray spectroscopy, and Brunauer–Emmett–Teller analysis were employed. Analysis revealed that the SI structure (choline chloride (ChCl)-citric acid) exhibited a higher surface area and pore volume compared to the SII structure (choline chloride (ChCl)-urea), while also demonstrating a smaller particle size. This difference can be attributed to the role of acidic eutectic solvents in metal oxide nanoparticle production. These results suggest that the SI structure demonstrates promising potential for adsorption and catalytic applications.

* **Corresponding author.**
E-mail address: m20.daraee@gmail.com

Cite this article as:

Daraee, M., Daraee, M., Feyzizadeh, A.,(2025). Roles of Acidic Deep Eutectic Solvents in Synthesis of Silica Nanoparticle. *Progress in Engineering Thermodynamics and Kinetics*. https://doi.org/10.22075/JPETK.2023.24860.1004

1. Introduction

The Earth's crust is mostly made up of silica (about 75%), a mineral found in abundance in ocean plates. Diatomaceous earth is a valuable source of this glassy form of silica [1]. Due to the promising specifications of silica nanoparticles (SNPs) in many fields, SNPs have gained much attention. Mesoporous silica nanoparticles have a regular structure with uniform pore size. Additionally, silica nanoparticles offer a range of advantages. These include a large surface area, which makes them useful for various applications; high thermal stability, meaning they can withstand high temperatures; chemical inertia, indicating they don't readily react with other chemicals; high hydrophilicity, meaning they attract water; biocompatibility, which makes them suitable for biological applications; weak permeability, allowing for controlled release of substances; great chemical versatility, meaning their surface chemistry can be easily modified; and finally, cost-effectiveness, making them an attractive option for many purposes [1, 2]. These characteristics of silica nanoparticles have encouraged industrial units to use them in many fields including heat insulators, noise suppressors, adhesives, aerogels, ink, paint, tire, and drug delivery system, cement, catalyst, adsorbent, construction sector, sensor, drug delivery, and polymer nanocomposites [3-16].

Various methods are employed to synthesize silica, depending on the desired type. Among these, the sol-gel method is particularly popular due to its ability to precisely control the size, distribution, and morphology of the resulting nanoparticles. This process comprises two distinct stages: hydrolysis and condensation. In the first stage, a colloidal suspension of particles forms within a liquid medium (a sol). In the second stage, these particles react with one another, forming an external polymer network that ultimately transforms into a gel. Two main classes of precursors are utilized in this method: inorganic compounds and alkoxides. Tetraethyl orthosilicate (TEOS) and sodium silicate are the most commonly used precursors [7,10].

Another process for the synthesis of silica is the one-step method, spray pyrolysis which considers as a metal precursor consists organic solvents solution with an oxidizing gas, is sprayed into a flame zone. In this method, the size and morphology of the nanoparticles depend on the precursor. Although sol-gel is a time-consuming synthesis method, due to its ability in the production of monodispersed particles, it is more common [2]. The sol-gel method is widely used for synthesizing silica nanoparticles. Mineral acid is commonly applied in silica production via the sol-gel [3]. Scientists are exploring environmentally friendly methods for nanoparticle production, and Deep Eutectic Solvents (DESs) represent a promising new avenue. While DESs and Ionic Liquids (ILs) share certain physical characteristics, their chemical properties differ significantly. A key advantage of DESs is their straightforward synthesis, achieved through the simple mixing of readily available components, unlike the more complex production of ILs. This mixing process generates unique properties, often stemming from Brønsted or Lewis acids and bases, that are not present in the individual starting materials. These emergent properties include high conductivity, strong intermolecular interactions, thermal stability, and negligible vapor pressure. These attributes render DESs highly attractive for a wide range of applications [17-19]. At present Deep Eutectic Solvents are widely used in the preparation of different nanomaterials [20-26]. In a research study, the synthesis of manganese oxide nanostructures was conducted for water purification and energy storage applications. Researchers aimed to develop a rapid, energy-efficient, solvent/reactant-free, and environmentally friendly method at room temperature. Using $KMnO_4$ as a precursor and various Deep Eutectic Solvents (DESs) – choline chloride (CC)-ethylene glycol (EG), CC-glucose, and CC-EG-glucose – as solvent-reducing agents, they achieved considerable results for detailed kinetics within 1 minute. Using CC-EG as a suitable compound for manganese oxide combination demonstrated higher flux performance for cationic dye removal and proved to be a good source of energy storage due to its high specific capacitance as an electroactive material [25].

In a research [24], metal oxides of $M_2V_2O_{7-\delta}$ (M = Zn and Cu) were obtained by surface photovoltage spectroscopy (SPS) in reaction with a deep eutectic solvent (DES), which is an eutectic mixture of a hydrogen bond donor (urea) and acceptor (choline chloride) in 2:1 mole ratio have formed the synthetic method for the first time which improved the high solubility of binary metal oxides in DES and increase mixing velocity of the metal precursors which could control the dimensions and composition of the products, and concentration of oxygen vacancies [24].

Despite limitations in solar energy conversion due to vanadates acting as electron/hole traps and recombination sites, deep eutectic solvents (DESs) hold significant promise for synthesizing semiconducting metal oxides with oxygen vacancies. Researchers explored the use of DESs as both solvents and inhibitors to rapidly synthesize crassula perforata-like TiO2 under mild conditions (160°C for 4-8 hours). Considering the prevalent use of ChCl/urea and ChCl/EG as DESs in nanomaterial synthesis, and their roles as solvents or templates, a ChCl/oxalic acid DES was prepared via a traditional method to reduce the hydrolysis rate of the titanium source in the TiO2 preparation process. This approach utilizes the combined effect of both hydrogen-bond donor and acceptor functionalities within the DES [27].

In another research, the Silica Gel Modified by Deep Eutectic Solvents and the BTEX adsorption efficiency was determined from gas streams. Adsorption performance was higher than unmodified SiO_2 [28]. However, the use of DESs in the nanoparticle's synthesis has not attracted much attention.

In this work, the synthesis of SiO_2 nanoparticles by Acidic DES is reported for the first time, by mixing the metal precursors and Acidic DES. Using acids, the DES can help to control the hydrolysis rate of silica source in the SiO_2 preparation process by the sol-gel method, so we selected citric acid as the H-bond donor to design and synthesize DES.

2. Experimental section

2.1. Materials

The SiO_2 was synthesized with starting materials following: Sodium silicate (pH value of 11–12, containing 7.5–8.5 % Na_2O and 25.5–28.5 % SiO_2 (≥ 99% purity)) was supplied by Merck Co. choline choloride (ChCl) (75%), urea, citric acid, H_2SO_4 were obtained from Chemical Reagent.

2.2. DESs preparation

A series of DESs were synthesized by mixing hydrogen-bond acceptors choline choloride (ChCl) with hydrogen-bond donors (citric acid and urea) with an acceptor to donor molar ratio of 1:1 and 1:2 at 90 °C for 1 h until clear, transparent, homogeneous target liquids appeared [29,30].

2.3. SiO_2 preparation with acidic eutectic solvents (ChCl-citric acid)

First, an acidic eutectic solvent (ChCl-citric acid) was added dropwise into a mixture containing 5 mL SS and 20 mL water under vigorous stirring. Subsequently, the resulting white mixture was transformed into a sol and then gelled. The addition of the acidic eutectic solvent was followed by stirring at room temperature for 30 minutes to achieve a pH of 3.5. Finally, after aging for 24 hours, the product was washed with distilled water and dried (100°C, 12 hours) to obtain silica nanoparticles. The synthesized SiO2 nanoparticles were labeled SI.

2.4. SiO_2 preparation with eutectic solvents (ChCl-urea)

The same procedure was repeated with eutectic solvents (ChCl-urea) and H_2SO_4 as a catalyst. The synthesized SiO_2 were labeled as SII. Figure 1 shows the schematic of the SiO_2 nanoparticles synthesis by DES.

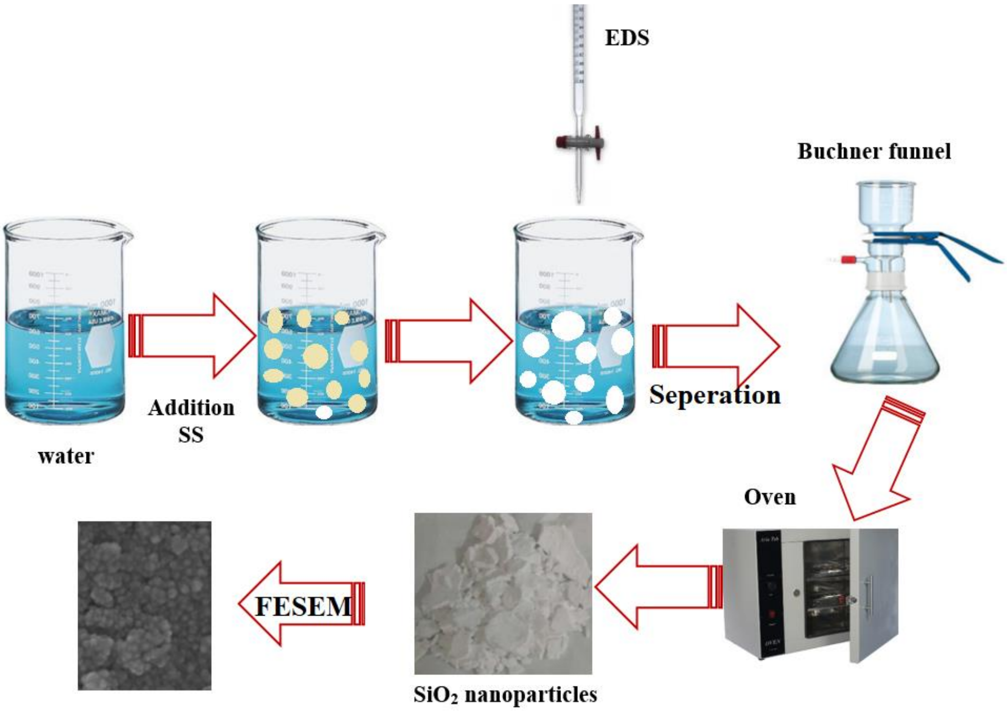

Fig.1. The schematic of the SiO_2 nanoparticles synthesis by DES.

3. Characterization

Characterization analyses were done on produced samples. i) X-Ray diffraction (XRD): A Bruker AXS-D8 Advance instrument was used to analyze the crystal structures of the samples by X-ray in the range of 10 to 80 degrees. The results reveal that how the atoms are arranged in the structure. ii) Fourier transform infrared (FTIR) spectroscopy: A Perkin Elmer-Spectrum 65 machine was used to identify the functional groups in the samples (4000-600 cm-1 range). This analysis shows how the samples absorb infrared light at different wavelengths. iii) Scanning electron microscopy (SEM): A VEGA3 TE-SCAN instrument was used to obtain the high-resolution images of the samples' surfaces, revealing their shapes and sizes. Surface area and porosity analysis: A nitrogen adsorption-desorption instrument was utilized to measure the surface area and porosity of the samples using the Brunauer–Emmett–Teller (BET) method. Prior to this analysis, the samples were degassed (removal of adsorbed gases) at 200°C for 2 hours. Pore size distribution**:** The Barrett–Joyner–Halenda (BJH) method was applied to the data obtained from the nitrogen adsorption-desorption experiment to determine the distribution of different pore sizes and their specific volumes within the samples.

4. Results and descussion

The synthesis and characterization of SiO_2 were investigated on two different DESs. It was schemed to prepare by employing choline chloride (Hydrogen bond donor), urea and acid citric (Hydrogen bond acceptor) to synthesize SiO_2 by exploiting SS as Si source.

Figure 2 shows the FTIR spectra of ChCl, urea, and the synthesized ChCl/Urea DES, and the optimized interaction structures between ChCl and urea. Figures 2a, 2b, and 2c show the spectra of Urea, ChCl, and ChCl-Urea, respectively. It has demonstrated that the characteristic spectrum of the ChCl-Urea constituted as the result of overlap of those urea and ChCl. In addition, the bands of ChCl, hydroxyl groups exist in 3210 cm^{-1} in the spectrum of ChCl. This band moved to 3315 cm^{-1} in ChCl-Urea. Also, bonds of ChCl such as CH and CCO appeared in ChCl-urea. These results reveal that the structure of CH was maintained in the ChCl-Urea. Particularly, the absorption bands of Urea at 3440 cm^{-1} and 3370 cm^{-1} , which can be attributed to the stretching mode of $-NH_2$, shifted towards the lower wavenumber region to 3423 cm^{-1} and 3356 cm^{-1}. This could be attributed to the forming of more hydrogen bonds between Urea and ChCl such as (O-H···N-H, O-H···O, and O-H···OH) [31,32].

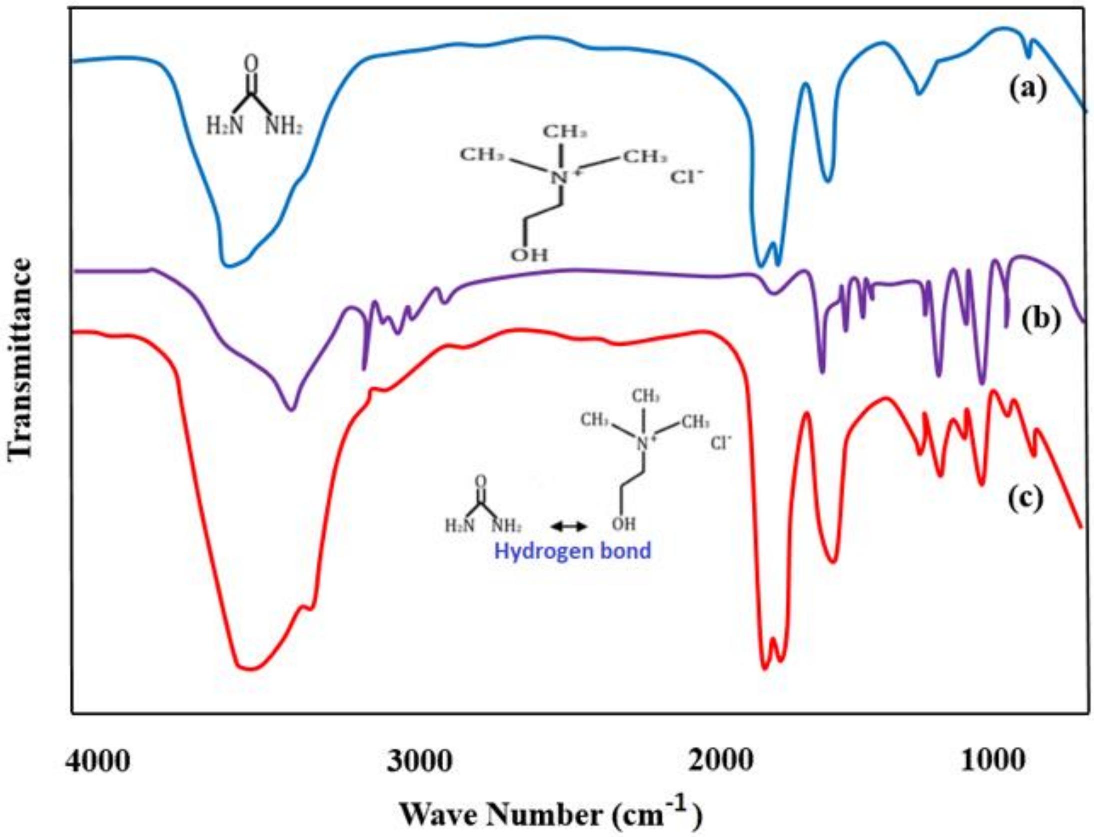

Fig.2. FTIR analysis: a) Urea, b) Chcl and c) Chcl-Urea.

Figure 3 is indicated the FTIR spectra of ChCl, citric acid, and the synthesized ChCl/citric acid DES. The vibrations for carbonyl in citric acid and hydroxyl in ChCl shows an obvious shift from 1683.11 to 1747.96 cm^{-1} and from 3227.54 to 3343.75 cm^{-1}, and the vibration for hydroxyl in citric acid simultaneously showed a shift from 3419.43 to 3343.75 cm^{-1}, which illustrates that the H-bonds were mainly formed between the hydrogen of hydroxyl in citric acid and ChCl.

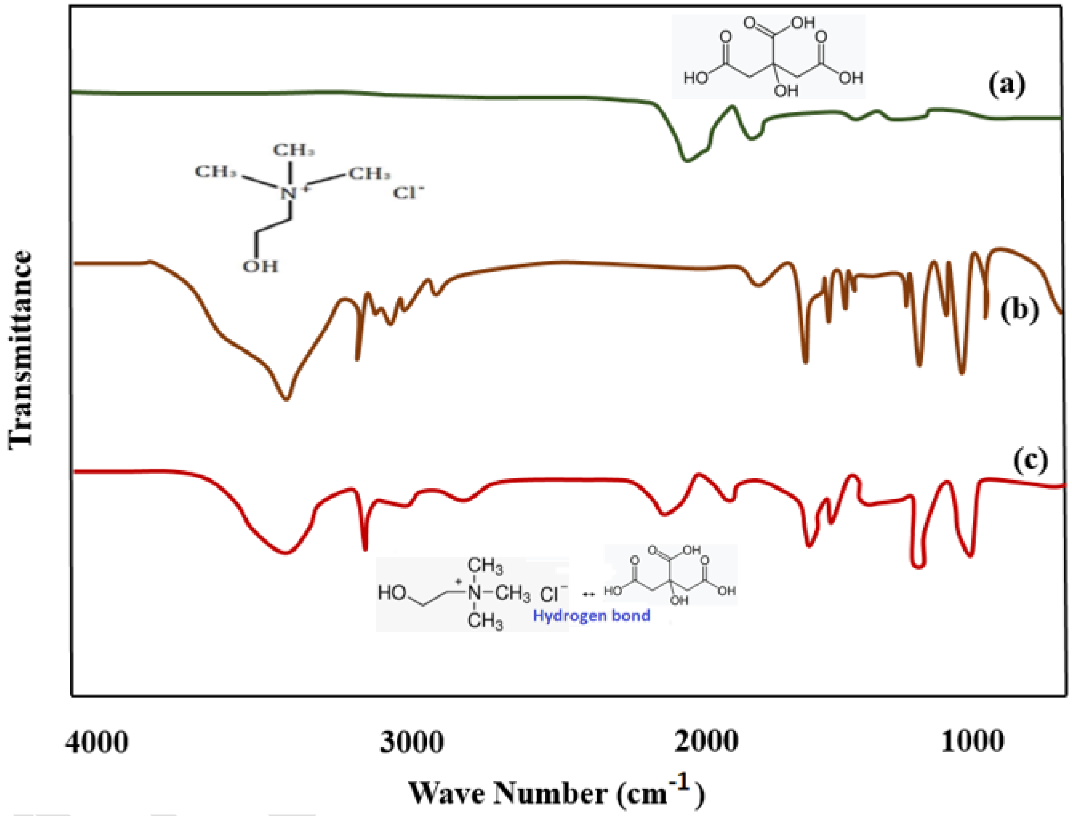

Fig. 3. The FTIR analysis of a) acid citric, b) Chcl and c) Chcl-acid citric.

In Figure 4, symmetric stretching vibrations and Si-O-Si asymmetric were emerged for all the silica (SI and SII) at 800 cm^{-1} and 1100 cm^{-1}, respectively. The peaks at 3421 cm^{-1}, 1630 cm^{-1} and 955 belong to O-H stretching, distorting vibrations. and vibration of Si-OH on silica particles, respectively [33-34].

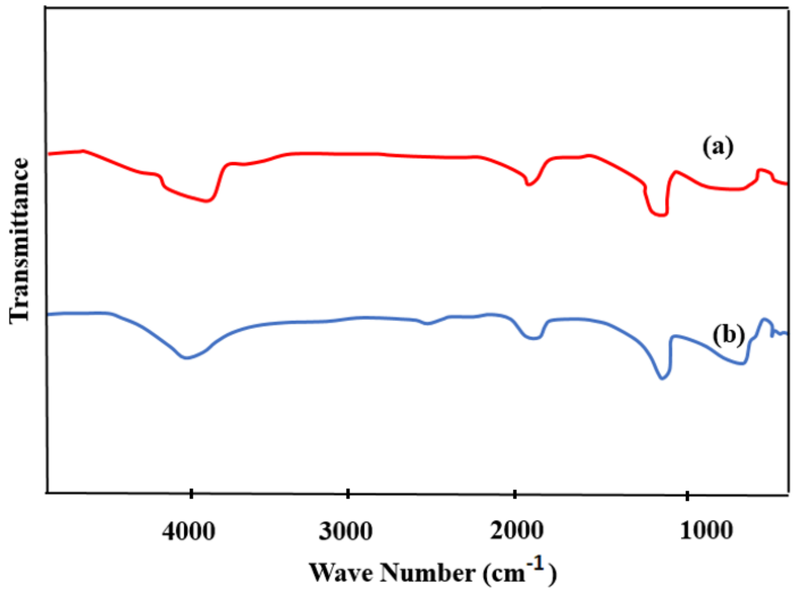

Fig. 4. The FTIR analysis of the a)SI b) SII nanoparticles.

The crystal structure and morphology of the synthesized nano-SiO_2 (SI and SII) were investigated using XRD. The diffraction pattern is shown in Figure 5, where a characteristic broad peak centered at 25° confirms its amorphous nature. Furthermore, it can be clearly seen that the average particle size of SI and SII was approximately 20-25 nm and 60-80 nm, respectively [33-34].

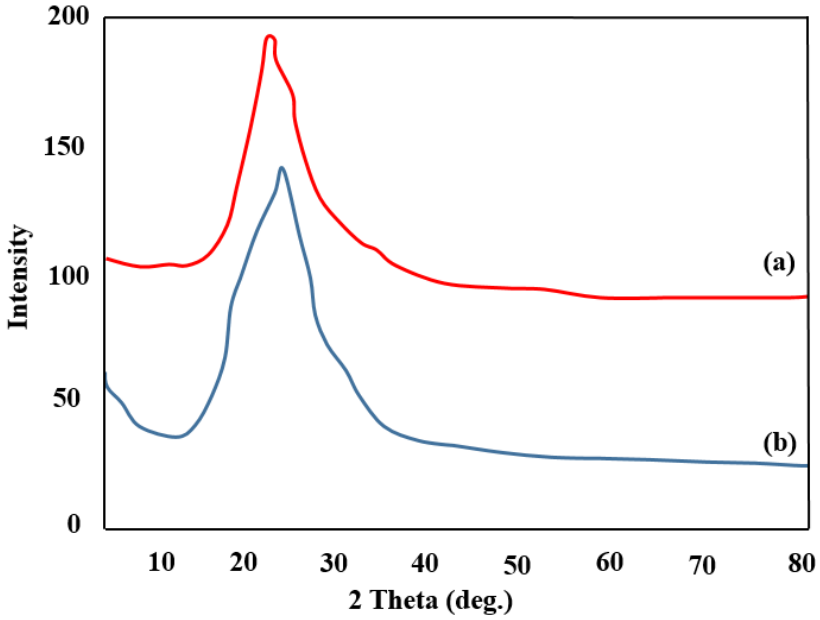

Fig. 5. The XRD pattern of the a)SI b) SII nanoparticles.

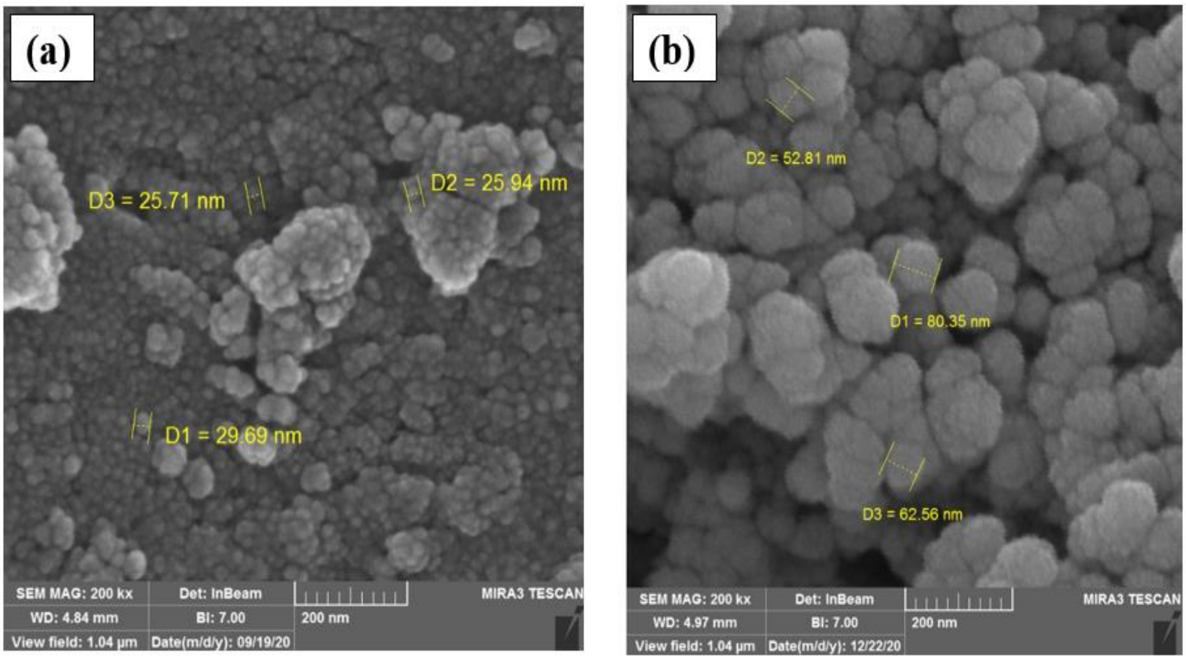

Fig. 6. The FESEM images of the a)SI, b) SII nanoparticles.

Figure 6 displays scanning electron microscopy (SEM) images of silica nanoparticles, prepared using two types of eutectic solvents, at the same magnification. The images reveal that the size of the resulting silica nanoparticles increased in S(II) compared to S(I) due to the inclusion of H_2SO_4, a strong mineral acid. Specifically, the presence of H_2SO_4 had an inverse effect on size, leading to larger particles in S(II) with an average diameter of 80 nm, compared to 25 nm for SI. Both samples exhibited spherical shapes. These observations highlight the significant influence of hydrogen-bond donor variations on SiO_2 size. When urea acts as the hydrogen-bond donor, adding H_2SO_4 as a catalyst promotes SiO_2 formation. In contrast, with citric acid as the hydrogen-bond donor, the acidic DES drives the formation of SiO_2. Notably, the hydrogen-bonded network within the DES acts as a templating agent during SiO_2 synthesis. Additionally, the presence of water facilitates the hydrolysis of SS, suggesting that the DES functions as both a solvent and a templating agent during the synthesis of SiO2 nanoparticles. [31,35].

Figure 7 and Table 1 show the EDS spectrum of amorphous SI particles with a smaller size. This spectrum exhibited only the presence of silicon and oxygen. The EDS spectrum did not show the presence of other elements.

Table 1. The EDS spectrum of amorphous SI nanoparticles.

Element	W%	A%
O	44.19	57.99
Si	53.99	42.01
Total	100.00	100.00

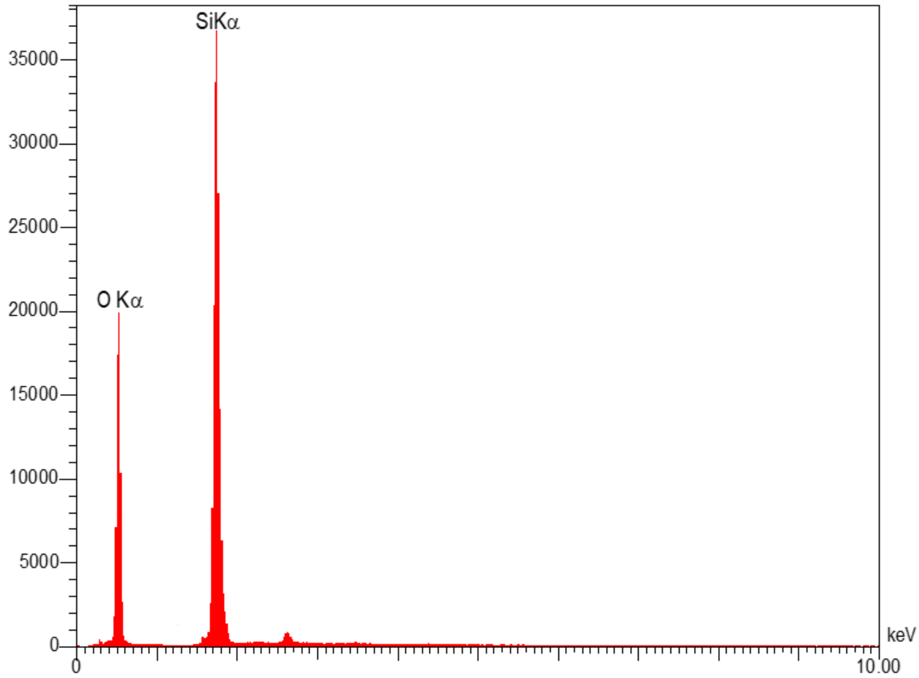

Fig. 7. The EDX analysis of the amorphous SI nanoparticles.

BET analysis was performed on the SI and SII silica structures. Determining the specific surface area is crucial for characterizing porous and finely dispersed solids, and gas adsorption offers the most suitable method for this task. When a gas comes into contact with a solid material, some of the gas molecules are adsorbed onto its surface. The amount of gas adsorbed depends on factors such as pressure, temperature, gas type, and surface area. By choosing appropriate measurement parameters (gas and temperature), the specific surface area can be reliably calculated from the resulting adsorption isotherm. For practical reasons, nitrogen adsorption at 77 K (liquid nitrogen temperature) is the established method for measuring specific surface area.

The term "BET method" refers to the analysis of isotherm data using a method developed by Brunauer, Emmett, and Teller. This method calculates the amount of gas adsorbed as a monolayer on the surface based on the measured isotherm. Multiplying this amount by the area per molecule gives the BET surface area. While nitrogen adsorption at 77 K is most common, krypton adsorption at 77 K is recommended for very small surface areas.

Figure 8 presents the nitrogen adsorption-desorption isotherms for SI and SII, while Table 2 summarizes the properties of the SiO_2 produced through this process. The SI and SII samples exhibited high surface areas (569 and 375 m²/g, respectively) and pore volumes (1.1 and 0.5 cm³/g, respectively). This suggests that SI structures may be suitable for various applications. All samples displayed characteristic Type IV isotherms with hysteresis loops according to IUPAC classification, indicating that the synthesized SiO_2 nanoparticles were mesoporous with narrow pore structures.

Figure 9 displays the pore size distribution (PSD) of SI and SII, obtained through the BJH method from the desorption branch. It is evident that the volume of nitrogen adsorbed by SiO_2 increased with the application of the acidic DES, due to the presence of hydrogen bonds. Meanwhile, the PSD shows that the SI and SII nanoparticles exhibited average pore diameters ranging from 5.8 nm and 7.8 nm, respectively.

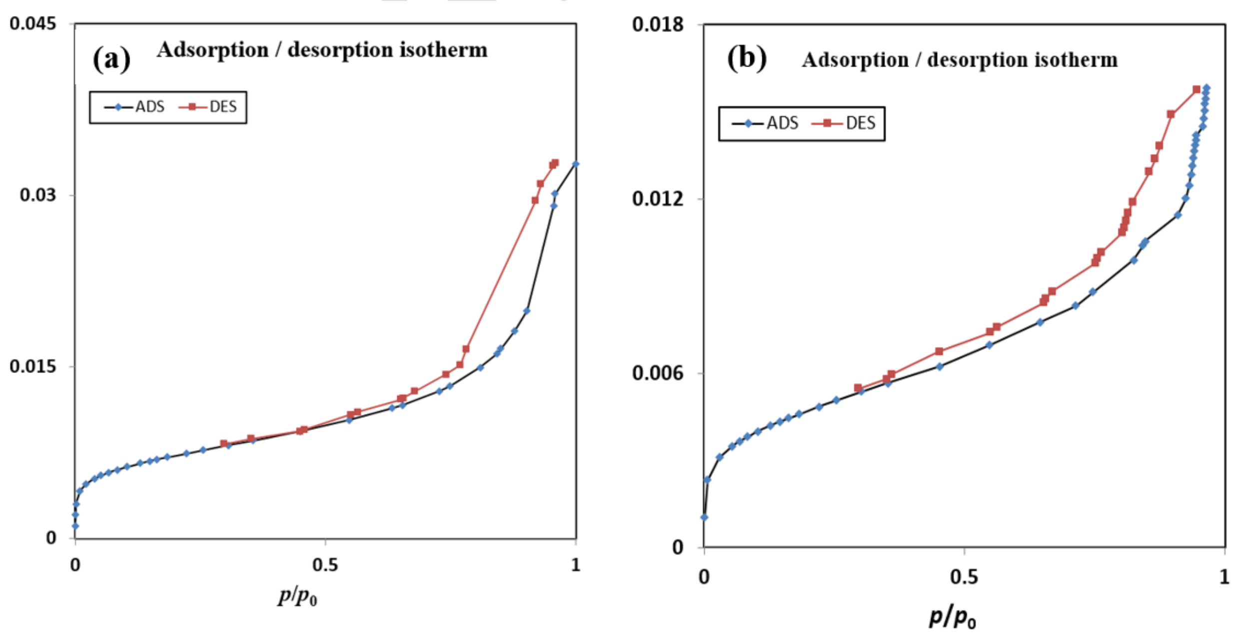

Fig. 8. Nitrogen adsorption/desorption isotherms of a) SI and SII nanoparticles.

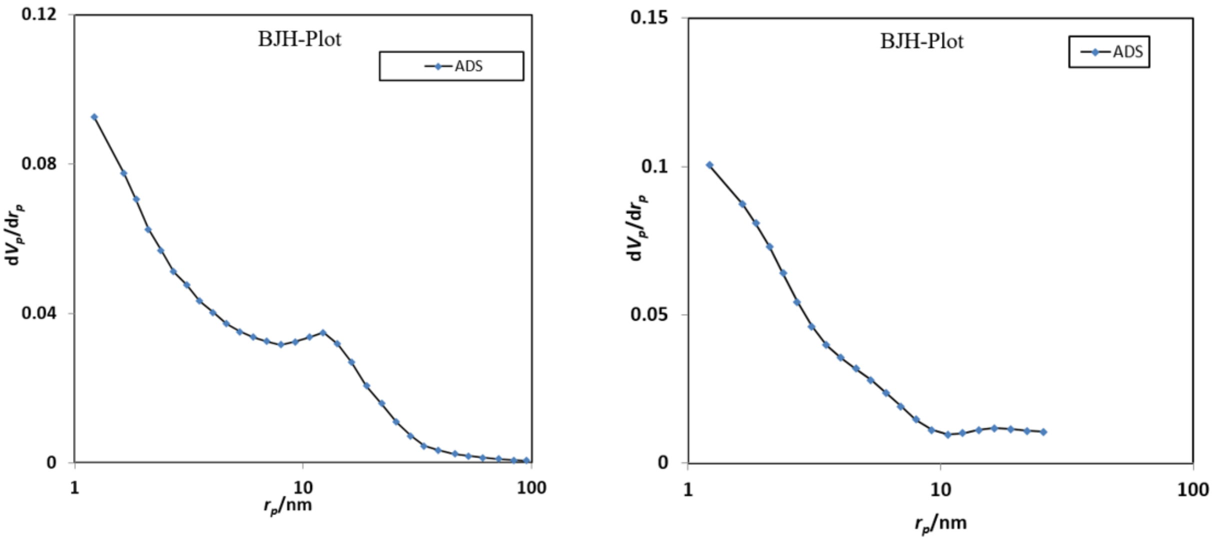

Fig. 9. Pore size distribution of a) SI, b) SII nanoparticles.

Table 2. Surface area and pore size distribution of SI and SII nanoparticles.

Sample	**Surface area (g/m^2)**	**Pore volume (g/cm^3)**	**Total Pore diameter (nm)**
SI	569	1.1	7.8
SII	375	0.5	5.8

5. Conclusion

This paper reports the first-time application of two deep eutectic solvents (DESs), ChCl-citric acid and ChCl-urea, to prepare silica nanoparticles (SiO_2) using the sol-gel method. The structures and properties of the prepared SiO_2 were characterized using FTIR, SEM, EDX, XRD, and BET techniques. Comparison of the two samples, SI and SII, revealed that the SI structure possessed a smaller particle size than SII. Additionally, analysis of the results demonstrated that the SI structure had a higher surface area and pore volume compared to SII. This difference can be attributed to the role of acidic eutectic solvents in influencing the production of metal oxide nanoparticles. Based on these findings, the SI structure shows promise as a candidate for adsorption and catalytic applications.

References

[1] M. Gonçalves, Sol-gel silica nanoparticles in medicine: A natural choice. Design, synthesis and products, Molecules. 23 (2018) 2021.

[2] L.P. Singh, et al., Sol-Gel processing of silica nanoparticles and their applications. Advances in colloid and interface science 214 (2014) 17-37.

[3] I.M. Joni, Rukiah, C. Panatarani, Synthesis of Silica Particles by Precipitation Method of Sodium Silicate: Effect of Temperature, pH and Mixing Technique, AIP Conference Proceedings., (2020).

[4] U. Zulfiqar, T. Subhani1, S. Wilayat Husain, Synthesis of silica nanoparticles from sodium silicate under alkaline conditions, J Sol-Gel Sci Technol 77 (2016) 753–758.

[5] C. Chapa-González, A.L. Piñón-Urbina, P.E. García-Casillas, Synthesis of Controlled-Size Silica Nanoparticles from Sodium Metasilicate and the Effect of the Addition of PEG in the Size Distribution, Materials (Basel) 11 (2018).

[6] M. Nabil, H.A. Motaweh, Shape control of silica powder formation. Journal of Materials Science and Chemical Engineering 7 (2019) 49-55.

[7] X. Jianga, X. Tang, L. Tang, et al., Synthesis and formation mechanism of amorphous silica particles via sol–gel process with tetraethylorthosilicate, Ceramics International 45 (2019) 7673–7680.

[8] S.N.M .Mestanza, A.O. Ribeiro, et al., Study of the influence of dynamics variables on the growth of silica nanoparticles. Inorganic and Nano-Metal Chemistry 47 (2017) 824-829.

[9] P.R. Monich, FV. Berti, L.M. Porto, B. Henriques, et al., Physicochemical and biological assessment of PEEK composites embedding natural amorphous silica fibers for biomedical applications, Materials Science and Engineering: C 79 (2017) 354–362.

[10] R.S. Dubey, Y.B.R.D. Rajesh, M.A. More, Synthesis and characterization of SiO_2 nanoparticles via sol-gel method for industrial applications, Materials Today: Proceedings (2015) 3575–3579.

[11] H. Mohamadi, M. Farahi, Preparation, characterization and catalytic application of nano-$Fe_3O_4@SiO_2@(CH_2)_3OCO_2Na$ as a novel basic magnetic nanocatalyst for the synthesis of new pyranocoumarin derivatives, RSC Advances 8 (2018) 27818-27824.

[12] Y. Cao, W. Zhai, X. Zhang, Sh. Li, et al., Mesoporous SiO2-supported Pt nanoparticles for catalytic appli cation. International Scholarly Research Notices 2013 (2013).

[13] H. Lv, T. Yan, X. Yang, J. Zhao, S. Liu, et al., Preparation and characterization of SiO2 nanowires using a SnO2 catalyst, Physics Letters A 384 (2020) 126174.

[14] T.T. Nguyen, H.T. Ma, P. Avti, M.J. Bashir, C.A. Ng, et al., Adsorptive removal of Iron using SiO2 nanoparticles extracted from rice husk ash, Journal of analytical methods in chemistry 2019 (2019).

[15] W-g. Kim, H.U. Kang, K-m. Jung, S.H. Kim, Synthesis of silica nanofluid and application to CO2 absorption, Separation Science and Technology 43 (2008) 3036-3055.

[16] F. Salaimi, K. Tahmasobi, Ch. Karami, A. Jahangiri, Preparation of Modified nano-SiO2 by Bismuth and Iron as a novel Remover of Methylene Blue from Water Solution, Journal of the Mexican Chemical Society 61 (2017).

[17] R. Xin, S. Qi, C. Zeng, F.I. Khan, B. Yang, Y. Wang, A functional natural deep eutectic solvent based on trehalose: Structural and physicochemical properties, Food Chemistry 217 (2017) 560-567.

[18] T.G. Kim, G.S. An, J.S. Han, J. Hur, P. bong-geun, S-C. Choi, Synthesis of Size Controlled Spherical Silica Nanoparticles via Sol-Gel Process within Hydrophilic Solvent, Journal of the Korean Ceramic Society 54 (2017) 49-54.

[19] E.L. Smith, A.P. Abbott, K.S. Ryder, Deep Eutectic Solvents (DESs) and Their Applications, Chemical Reviews 114 (2014) 11060-11082.

[20] M. Aghazadeh, F. Aghazadeh, Effects of deep eutectic solvents in preparation of nanoparticles TiO, Int. J. Bio-Inorg. Hybr. Nanomater 6 (2017) 215-220.

[21] D. Hu, Y. Xie, L. Liu, P. Zhou, J. Zhao, et al., Constructing TiO2 nanoparticles patched nanorods heterostructure for efficient photodegradation of multiple organics and H2 production, Applied Catalysis B Environmental 188 (2016) 207–216.

[22] J. Richter, M. Ruck, Synthesis and dissolution of metal oxides in ionic liquids and deep eutectic solvents, Molecules 25 (2020) 78.

[23] M. Karimi, M.J. Eshraghi, V. Jahangir, A facile and green synthetic approach based on deep eutectic solvents toward synthesis of CZTS nanoparticles, Materials Letters 171 (2016) 100–103.

[24] S. Hong, R.M. Doughty, F. Osterloh, J.V. Zaikina, Deep eutectic solvent route synthesis of zinc and copper vanadate n-type semiconductors-mapping oxygen vacancies and their effect on photovoltage, Journal of Materials Chemistry A 7 (2019) 12303-12316.

[25] K. Aruchamy, N. Maalige R, M. Halanur M, A. Mahto, R. Nagaraj, et al., Ultrafast synthesis of exfoliated manganese oxides in deep eutectic solvents for water purification and energy storage, Chemical Engineering Journal 379 (2020) 122327.

[26] Q. Wang, B. Dong, Y. Zhao, F. Huang, J. Xie, G. Cui, B. Tang, Controllable green synthesis of crassula peforata-like TiO2 with high photocatalytic activity based on deep eutectic solvent (DES), Chemical Engineering Journal 348 (2018) 811-819.

[27] A. Abbott, G. Capper, D.L. Davies, K. McKenzie, S.U. Obi, Solubility of Metal Oxides in Deep Eutectic Solvents Based on Choline Chloride, Journal of Chemical and Engineering Data - J CHEM ENG DATA 51 (2006) 1280-1282.

[28] P. Makoś, E. Słupek, A. Małachowska, Silica Gel Impregnated by Deep Eutectic Solvents for Adsorptive Removal of BTEX from Gas Streams, Materials Basel, Switzerland 13 (2020).

[29] N. Azizi, M. Edrisi, Z. Manochehri, Greenersynthesisof magnetic nanoparticles in an aqueous deepeutectic solvent, Scientia Iranica, 23 (2016) 2750-2755.

[30] Z. Maugeri, P.D. de María, Novel choline-chloride-based deep-eutectic-solvents with renewable hydrogen bond donors: Levulinic acid and sugar-based polyols, RSC Adv 2 (2011) 421-425.

[31] C. Du, B. Zhao, X.B. Chen, N. Birbilis, H. Yang, Effect of water presence on choline chloride-2urea ionic liquid and coating platings from the hydrated ionic liquid, Scientific reports 6 (2016) 29225.

[32] J.-S. Lee, Deep eutectic solvents as versatile media for the synthesis of noble metal nanomaterials, Nanotechnology Reviews 6 (2017) 271-278.

[33] S. Sekar, G. Antony a, V. Vijayan, L. Marappan, S. Baskar, Synthesis of SiO_2 nano particles by using sol-gel route, International Journal of Mechanical Engineering and Technology (2019) 785-790.

[34] R.S. Dubey, Y.B.R.D. Rajesh, M.A. More, Synthesis and Characterization of SiO_2 Nanoparticles via Sol-gel Method for Industrial Applications, Materials Today: Proceedings, (2015) 3575-3579.

[35] O. Gomez Rojas, The role of ionic liquids/deep eutectic solvents in sol-gel syntheses of complex metal oxides, in, University of Bristol, (2019).